American Mineralogist, Volume 91, pages 385–393, 2006

The partial molar volume of Fe_2O_3 in alkali silicate melts: Evidence for an average Fe^{3+} coordination number near five

QIONG LIU* AND REBECCA A. LANGE

Department of Geological Sciences, University of Michigan, 2534 C.C. Little Building, Ann Arbor, Michigan 48109-1005, U.S.A.

ABSTRACT

High-temperature (867–1534 ºC) density measurements were performed in air on 10 liquids in the Na_2O-Fe_2O_3-FeO-SiO_2 (NFS) system and 5 liquids in the K_2O-Fe_2O_3-FeO-SiO_2 (KFS) system using Pt double-bob Archimedean method. Replicate measurements indicate an average reproducibility of 0.22%. Compositions (in mol%) range from 4 to 18 Fe_2O_3, 0 to 3 FeO, 18 to 39 Na_2O, 25 to 37 K_2O, and 43 to 67 SiO_2. Errors in the gram formula weight are ~0.4%. The molar volumes were fitted to a linear compositional model, which gives a compositionally independent partial molar volume ($\pm 2\sigma$) for the Fe_2O_3 component ($\overline{V}_{Fe_2O_3}$) of 41.52 ± 0.34 cm^3/mol and zero thermal expansivity. The average residual to the fit is ±0.36% for our 57 measurements on 15 liquids at various temperatures. The value for $\overline{V}_{Fe_2O_3}$ in silicate liquids when Fe^{3+} is in fourfold vs. sixfold coordination is estimated to be ~45.5 ± 1 vs. ~34 ± 1 cm^3/mol, respectively. Thus, the fitted value of 41.5 cm^3/mol appears to reflect an average Fe^{3+} coordination number between 4.5 and 5.0, which is consistent with recently published X-ray absorption fine structure (XAFS) spectroscopy and molecular dynamics (MD) simulations on Fe^{3+}-bearing silicate glasses. In the literature, $^{V}Fe^{3+}$ is inferred to be present in trigonal bipyramidal sites, in contrast to the square pyramidal sites for $^{V}Ti^{4+}$. The lack of a strong compositional or temperature dependence for $\overline{V}_{Fe_2O_3}$ in these alkaline silicate liquids, in contrast to what is observed in the literature for $\overline{V}_{TiO_2}$ in similar melts, may reflect the different geometries for $^{V}Fe^{3+}$ and $^{V}Ti^{4+}$.

INTRODUCTION

Iron is the only major element in natural silicate melts with more than one oxidation state. To model magmatic processes, thermodynamic descriptions of silicate melts must include precise information on both the Fe_2O_3 and FeO components. The structural role of Fe_2O_3 and FeO in magmatic liquids strongly influences how the Fe-redox ratio varies as a function of composition, temperature, pressure, and oxygen fugacity. Although it has long been known that Fe^{3+} may occur in both four- and sixfold coordination in silicate glasses, only recently has a five-coordinated geometry around Fe^{3+} been confirmed in silicate glasses at one bar utilizing X-ray absorption fine structure (XAFS) spectroscopy and molecular dynamics (MD) simulations (Farges et al. 2004).

Because the density of a magmatic liquid is largely determined by the geometrical packing of its network-forming cations (e.g., Si^{4+}, Al^{3+}, Ti^{4+}, and Fe^{3+}), the capacity of Fe^{3+} to undergo composition-induced coordination changes affects the partial molar volume of the Fe_2O_3 component, which must be known to calculate how the Fe^{3+}/Fe^{2+} values in magmatic liquids changes with pressure. The ferric/ferrous ratio in turn allows variations in the oxygen fugacity of magmatic liquids to be calculated as a function of depth in the mantle (Kress and Carmichael 1991). In addition, it is well established that Fe^{3+}/Fe^{2+} equilibrium behaves differently in calcic vs. sodic vs. potassic vs. natural liquids (e.g., Thornber et al. 1980; Sack et al. 1980; Kress and Carmichael 1988, 1989; Lange and Carmichael 1989; Tangeman et al. 2001). Some of these differences may be caused by changes in the coordination environment of Fe^{3+} in these various liquids (e.g., Nishida et al. 1981; Mysen 1987).

The capacity of Fe^{3+} to occur in variable coordination environments (4, 5, and 6) in silicate liquids at one bar is a feature it shares with Ti^{4+} (e.g., Farges et al. 1996a, 1996b, 1996c; Farges 1997). Moreover, both Fe_2O_3- and TiO_2-bearing alkali silicate liquids display anomalous configurational contributions to their heat capacity immediately above the glass transition (Richet and Bottinga 1985; Lange and Navrotsky 1993; Tangeman and Lange 1998; Bouhifd et al. 1999). Therefore, one of the goals of the present study was to explore further both the similarities and differences between the volumetric properties of Fe_2O_3- and TiO_2-bearing alkali silicate liquids. Liu and Lange (2001) found that there is a remarkably linear and systematic variation in $\overline{V}_{TiO_2}$ and $\partial\overline{V}_{TiO_2}/\partial T$ with Na_2O and K_2O content, which they related to a systematic shift in average Ti^{4+} coordination. In this study, we test whether a similar trend is observed in Fe_2O_3-bearing alkali silicate liquids.

Previous work on the density of Fe^{3+}-bearing alkali silicate liquids has been restricted to sodic liquids. Mo et al. (1982) and Lange and Carmichael (1987) each measured the density of acmite (or aegirine, $NaFeSi_2O_6$) liquid, which has an Fe^{3+}/Fe^{2+} value that varies with temperature. Dingwell et al. (1988) measured 11 sodium iron silicate liquids, one of which is also $NaFeSi_2O_6$. In this study, we measured the density of 10 additional sodic liquids (including $NaFeSi_2O_6$) as well as 5 potassic liquids. Our attempts to measure the density of $KFeSi_2O_6$ liquid (Fe-leucite

* E-mail: qiongl@umich.edu

0003-004X/06/0203–385$05.00/DOI: 10.2138/am.2006.1902

from Tangeman et al. 2001) and NFS-8 liquid (from Lange and Carmichael 1989) were unsuccessful owing to their high viscosity and are not reported.

EXPERIMENTAL METHODS

Sample synthesis and compositional analysis

Six of the 10 Na_2O-Fe_2O_3-FeO-SiO_2 samples investigated in this study (NFS-1, -2, -3, -4, -5, -6) are from Lange and Carmichael (1989), and the 5 K_2O-Fe_2O_3-FeO-SiO_2 samples (KFS-2, -3, -4, -5, -6) are from Tangeman et al. (2001). All of these samples were analyzed by wet-chemical methods. Four additional Na_2O-Fe_2O_3-FeO-SiO_2 samples (NFS-9, -10, -11, -12) were synthesized by mixing appropriate proportions of reagent grade Na_2CO_3, Fe_2O_3, and SiO_2. The compositions of these four samples were designed specifically to test the effect of varying the Na:Si ratio at constant total Fe concentration; one of these (NFS-10) is acmite ($NaFeSi_2O_6$) liquid. The mixed powders were dried slowly and de-carbonated, and then fused at 1273–1673 K. The samples were quenched to glasses, ground to a powder, and re-fused. To ensure sample homogeneity, this procedure was repeated twice.

The four samples synthesized in this study (NFS-9, -10, -11, -12) were each quenched to a glass, and analyzed with a Cameca Camebax electron microprobe at the University of Michigan. Standard operating conditions consisted of a focused electron beam in raster mode, an accelerating voltage of 15 kV, and beam current of 4.9 nA. Standards included two Na_2O-Fe_2O_3-FeO-SiO_2 glasses (NFS-2 and NFS-5) that were analyzed by wet-chemical methods, and were reported in Lange and Carmichael (1989). All analyses are listed in Table 1a and depicted on Figure 1.

For each composition, the gram formula weight (gfw = $\Sigma X_i MW_i$) is tabulated, where X_i is the mole fraction of each oxide component, and MW_i is the molecular weight of each oxide component. The average error on the gram formula weight is ~0.4% for those analyzed by wet chemistry as well as those analyzed with the electron microprobe using the wet chemically analyzed glass standards.

High-temperature measurements of liquid volume

Fifty-seven high-temperature, liquid density measurements were made on the 15 samples using the Pt double-bob Archimedean method (see Liu and Lange 2001, for a detailed description). Briefly, the sample liquids were held (~3 cm depth) in a Pt crucible that was placed inside a vertical tube Deltech furnace on a platform. The furnace was moved up and down with the action of a hydraulic jack. An electronic balance with a precision of ±0.0001 g was mounted on an aluminum shelf atop the furnace to measure the mass of the Pt bob before and after immersion into each experimental liquid. By using at least two Pt bobs of different mass (26.6 and ~11.6 g), but identical stem diameters, the effect of surface tension is eliminated. Two bobs (one large and one small) allow a single density measurement to be made, whereas four bobs (two different large bobs and two different small bobs) allow four density measurements to be made at each temperature.

Measurements were made at three to four different temperatures for each sample, spanning an interval that ranged from 93 to 393°. The lower temperature limits of the density experiments were constrained by the liquidus temperatures and melt viscosities (the double-bob Archimedean method is optimal when melt viscosities are $\leq 10^4$ Pa-s), whereas the upper limit was constrained to temperatures where alkali loss was insignificant. Replications at lower temperatures, after the highest temperature measurements were made, show no systematic deviation that may be attributable to alkali loss.

The accuracy of the results was tested by performing density measurements on NaCl liquid at 1194 and 1298 K (Table 2; Fig. 2). Our measurements are similar to those of Liu and Lange (2001), Lange and Carmichael (1987), and Stein et al. (1986), and are within –0.34 and –0.07% of the values recommended by NIST (Janz 1980).

TABLE 1A. Composition of samples from this study (wt%)

Sample	SiO_2	Fe_2O_3(total)	Na_2O	K_2O	Total
NFS-1	32.09	36.62	30.32		99.03
NFS-2	41.11	26.86	31.64		99.61
NFS-3	49.90	16.46	33.00		99.36
NFS-4	50.42	21.94	28.15		100.51
NFS-5	61.15	10.80	28.29		100.24
NFS-6	57.55	19.90	22.03		99.48
NFS-9*	45.00	35.03	20.06		100.09
NFS-10*	50.95	34.27	14.46		99.68
NFS-11*	41.11	35.01	24.27		100.39
NFS-12*	37.41	34.64	27.99		100.04
KFS-2	35.10	23.70		40.66	99.46
KFS-3	41.96	14.07		43.76	99.79
KFS-4	43.25	18.67		37.52	99.44
KFS-5	53.16	9.78		37.37	100.31
KFS-6	51.69	17.94		31.05	100.68
LC-25†	52.29	34.00	13.57		99.86

Note: Wet chemical analyses from Lange and Carmichael (1989) and Tangeman et al. (2001).
* Probe analysis from the University of Michigan.
† The original wt% data are reported here because only mol% was reported in Lange and Carmichael (1987).

TABLE 1B. Compositions of samples from Dingwell et al. (1988) (wt%)

Sample	SiO_2	Fe_2O_3(total)	Na_2O	Total
DBD-1	62.04	27.73	10.31	100.08
DBD-2	52.82	35.22	12.65	100.69
DBD-3	44.29	40.15	16.55	100.99
DBD-4	40.61	42.75	19.21	102.57
DBD-5	43.95	34.63	22.71	101.29
DBD-6	49.46	25.93	25.77	101.16
DBD-7	52.86	17.66	29.52	100.04
DBD-9	38.49	25.98	34.45	98.92
DBD-10	32.76	36.85	30.72	100.33
DBD-11	29.54	44.36	28.30	102.20
DBD-12	22.68	55.34	24.77	102.79

RESULTS

Density of the NFS and KFS liquids

Our density data on 10 liquids in the Na_2O-Fe_2O_3-FeO-SiO_2 (NFS) system and 5 liquids in the K_2O-Fe_2O_3-FeO-SiO_2 (KFS) system are presented in Table 3. For those samples where replicate density measurements were made, the standard deviations range from 0.04 to 0.81%, with an average reproducibility of 0.22%. These density data were converted to molar volumes by dividing into the gram formula weight:

TABLE 2. Density of molten NaCl (g/cm³)

Temperature (K)	Data	Mean
1194	1.488	
1194	1.484	
1194	1.489	
1194	1.484	
		1.486 ± 0.003
1298	1.432	
1298	1.435	
		1.434 ± 0.002

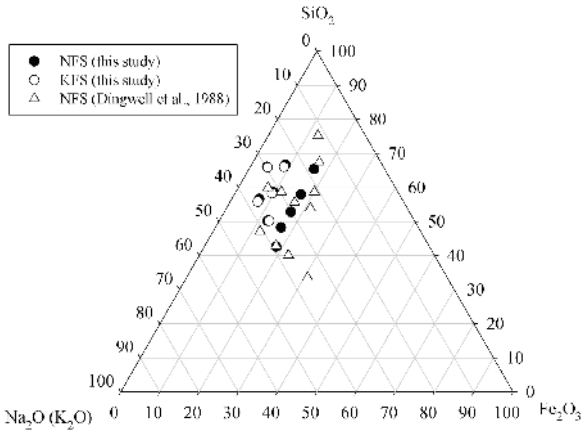

FIGURE 1. Composition of the experimental liquids in Na_2O-SiO_2-Fe_2O_3(total) and K_2O-SiO_2-Fe_2O_3(total) ternary systems (mol%).

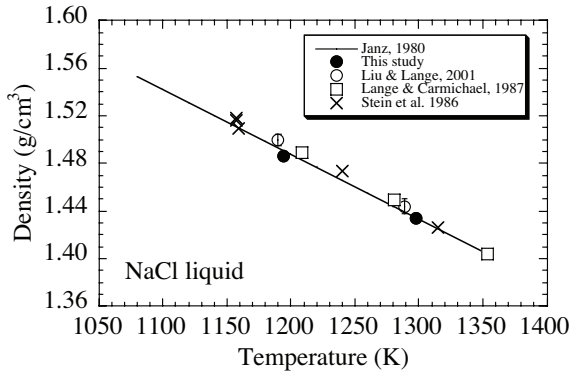

FIGURE 2. The density of NaCl liquid as a function of temperature. The equation from Janz (1980) is shown as a solid line [$\rho = 2.139 - 5.43 \times 10^{-4} T$ (K)]. Data points are from Stein et al. (1986), Lange and Carmichael (1987), Liu and Lange (2001), and this study.

$$V(T) = \mathrm{gfw}(T)/\rho(T) \quad (1)$$

Because the composition (and thus the gram formula weight) of Fe-bearing liquids varies with temperature, the compositions of all samples at their respective temperature of density measurement are also shown in Table 3. Values of Fe_2O_3/FeO in the NFS and KFS liquids were calculated at each temperature of measurement with the model equations of Lange and Carmichael (1989) and Tangeman et al. (2001), respectively. A propagation of experimental errors, including those from the compositional analyses, indicates a maximum error of ~1% and an average uncertainty of ~0.4% in the molar volumes.

Inter-laboratory comparison

The various measurements on acmite ($NaFeSi_2O_6$) liquid, which was synthesized, analyzed, and its density measured in four independent studies (Mo-002 from Mo et al. 1982; LC-25 from Lange and Carmichael 1987; DBD-2 from Dingwell et al. 1988; and NFS-10 from this study), allow an inter-laboratory comparison to be made. These data are compared in a plot of density vs. temperature in Figure 3a. The results show that the temperature dependence of density for NFS-10, LC-25, and Mo-002 are all similar, but the densities differ. The slope of density vs. temperature for DBD-2 liquid is less well defined. At 1673 K, the density of NFS-10 differs from that of DBD-2, LC-25, and Mo-002 by 0.11, 0.84, and 1.38%, respectively. However, part of this variation in density may be related to compositional differences. In Table 4, the compositions of these four liquids at 1673 K are shown along with their gram formula weights, which allow the molar volumes to be calculated and compared (Fig. 3b). In this case, at 1673 K, the molar volume of NFS-10 differs from that of DBD-2, LC-25, and Mo-002 by 0.18, 0.51, and 1.48%, respectively. Note that the molar volumes for NFS-10, LC-25, and Mo-002 decrease with temperature (Fig. 3b), which is the expected trend owing to the decrease of the Fe_2O_3/FeO ratio in the liquid with temperature. This decrease causes the gram formula weight for each liquid to decrease with temperature more rapidly than density, and results in molar volumes that decrease with temperature. Because the molar volume of Mo-002 deviates from the other acmite liquids by an amount (up to 1.48%) that is outside the reported errors, this sample is not included in the regression considered below.

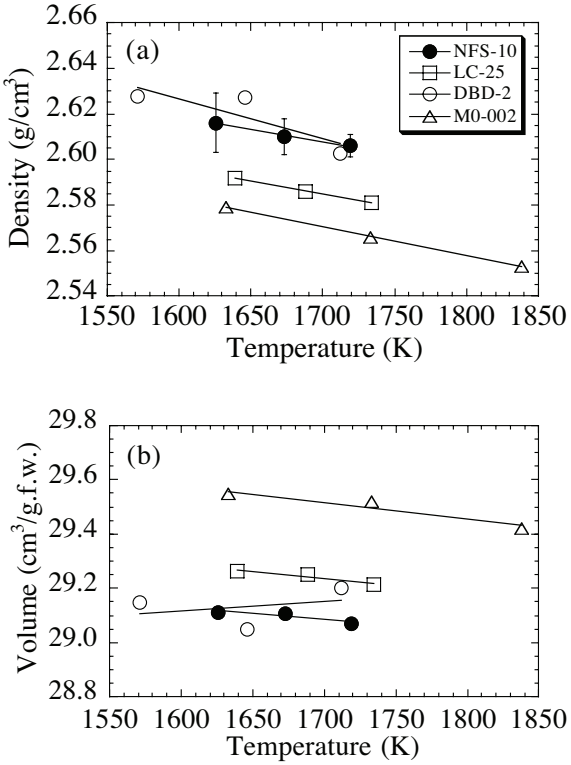

FIGURE 3. (**a**) Plot of density vs. temperature for four different acmite liquids. Data points of Mo-002, DBD-2, LC-25, and NFS-10 are from Mo et al. (1982), Dingwell et al. (1988), Lange and Carmichael (1987), and this study respectively. (**b**) Plot of molar volume vs. temperature for four different acmite liquids. Symbols are the same as in **a**.

A linear fit to the data

The liquid volume data for the Na_2O-Fe_2O_3-FeO-SiO_2 and K_2O-Fe_2O_3-FeO-SiO_2 liquids in Table 3 were combined with density data from the literature on Na_2O-Fe_2O_3-FeO-SiO_2 liquids (Dingwell et al. 1988; Lange and Carmichael 1987) and K_2O-Na_2O-SiO_2 liquids (Bockris et al. 1956; Stein et al. 1986; Lange and Carmichael 1987; Lange 1996, 1997) to calibrate the following linear volume equation:

$$V^{\mathrm{liq}}(X,T) = \sum X_i \left\{ \overline{V}_{i,T_{\mathrm{ref}}} + \partial \overline{V}_{i,T_{\mathrm{ref}}} / \partial T \left(T - T_{\mathrm{ref}}\right) \right\} \quad (2)$$

where X_i is the mole fraction of each oxide component, $\overline{V}_{i,T_{\mathrm{ref}}}$ is the partial molar volume of each oxide component at a reference temperature (T_{ref} = 1673 K), and $\partial \overline{V}_{i,T_{\mathrm{ref}}}/\partial T$ is the partial molar expansivity of each oxide component. The values for the fitted partial molar volumes and thermal expansivities for SiO_2, Na_2O, and K_2O are shown in Table 5 and are within error of those reported in Lange (1997). The fitted value ($\pm 2\sigma$) for $\overline{V}_{Fe_2O_3}$ is 41.52 ± 0.34, whereas the fitted value for $\partial \overline{V}_{Fe_2O_3}/\partial T$ is indistinguishable from zero, and so it was dropped from the regression of Equation 2.

The residuals for our 57 density measurements on 15 liquids at various temperatures range from +1.00 to –0.98%, with an

TABLE 3. Density, composition, and volume of experimental liquids

Sample	T (K)	Density (g/cm³)	S.D. %	X_{SiO_2}	$X_{Fe_2O_3}$	X_{FeO}	X_{Na_2O}	X_{K_2O}	gfw.	V_{meas} (cm³/gfw)	V_{calc} (cm³/gfw)	% Residuals 100 × (meas-calc)/meas
NFS-1	1290	2.680		0.4262	0.1827	0.0007	0.3903		79.024	29.487	29.197	0.98
NFS-1	1390	2.658		0.4259	0.1821	0.0020	0.3900		78.985	29.716	29.482	0.79
NFS-2	1140	2.621		0.5020	0.1234	0.0001	0.3746		73.093	27.887	27.895	–0.03
NFS-2	1240	2.589		0.5019	0.1232	0.0003	0.3745		73.063	28.221	28.180	0.14
NFS-2	1342	2.559		0.5017	0.1229	0.0009	0.3744		73.040	28.542	28.469	0.26
NFS-2	1440	2.535		0.5013	0.1222	0.0023	0.3741		72.986	28.791	28.730	0.21
NFS-2	1533	2.519 ± 0.001	0.04	0.5006	0.1209	0.0050	0.3735		72.893	28.937	28.952	–0.05
NFS-3	1240	2.476		0.5664	0.0702	0.0002	0.3632		67.767	27.370	27.408	–0.14
NFS-3	1342	2.455		0.5663	0.0700	0.0006	0.3631		67.752	27.597	27.693	–0.34
NFS-3	1440	2.436		0.5661	0.0696	0.0014	0.3629		67.721	27.800	27.957	–0.56
NFS-3	1533	2.412		0.5656	0.0688	0.0030	0.3626		67.660	28.051	28.190	–0.50
NFS-4	1240	2.531 ± 0.003	0.12	0.5864	0.0959	0.0003	0.3175		70.248	27.755	27.831	–0.27
NFS-4	1342	2.507		0.5862	0.0956	0.0008	0.3174		70.218	28.009	28.073	–0.23
NFS-4	1440	2.492		0.5859	0.0950	0.0019	0.3172		70.170	28.158	28.295	–0.48
NFS-4	1533	2.474 ± 0.004	0.16	0.5852	0.0940	0.0041	0.3168		70.102	28.335	28.487	–0.53
NFS-4	1625	2.467		0.5840	0.0921	0.0079	0.3161		69.956	28.357	28.639	–1.00
NFS-5	1342	2.394		0.6600	0.0437	0.0004	0.2959		65.002	27.152	27.310	–0.58
NFS-5	1440	2.378 ± 0.003	0.13	0.6598	0.0434	0.0009	0.2959		64.978	27.325	27.528	–0.74
NFS-5	1533	2.359 ± 0.003	0.13	0.6594	0.0429	0.0020	0.2957		64.941	27.529	27.724	–0.71
NFS-5	1625	2.339 ± 0.002	0.09	0.6588	0.0420	0.0038	0.2954		64.872	27.735	27.902	–0.60
NFS-6	1342	2.482		0.6658	0.0963	0.0007	0.2471		70.748	28.504	28.354	0.53
NFS-6	1440	2.463		0.6654	0.0858	0.0018	0.2470		69.120	28.063	28.111	–0.17
NFS-6	1553	2.449		0.6647	0.0848	0.0038	0.2467		69.043	28.192	28.290	–0.35
NFS-6	1625	2.434		0.6634	0.0830	0.0074	0.2462		68.905	28.309	28.357	–0.17
NFS-9	1394	2.639 ± 0.016	0.61	0.5790	0.1687	0.0021	0.2502		77.387	29.324	29.247	0.26
NFS-9	1486	2.627 ± 0.019	0.72	0.5790	0.1674	0.0048	0.2498		77.348	29.444	29.400	0.15
NFS-9	1579	2.608 ± 0.021	0.81	0.5763	0.1649	0.0097	0.2490		77.089	29.559	29.453	0.36
NFS-9	1673	2.592 ± 0.020	0.77	0.5733	0.1606	0.0185	0.2477		76.774	29.620	29.467	0.51
NFS-10	1626	2.616 ± 0.013	0.50	0.6466	0.1556	0.0200	0.1778		76.155	29.111	29.124	–0.04
NFS-10	1673	2.610 ± 0.008	0.31	0.6446	0.1532	0.0249	0.1773		75.973	29.108	29.094	0.05
NFS-10	1719	2.606 ± 0.005	0.19	0.6425	0.1504	0.0304	0.1767		75.758	29.070	29.050	0.07
NFS-11	1244	2.689 ± 0.010	0.37	0.5282	0.1691	0.0004	0.3023		77.505	28.823	28.935	–0.39
NFS-11	1346	2.642 ± 0.007	0.26	0.5279	0.1686	0.0013	0.3022		77.466	29.321	29.159	0.55
NFS-11	1441	2.616 ± 0.005	0.19	0.5273	0.1677	0.0032	0.3018		77.398	29.586	29.347	0.81
NFS-11	1532	2.603 ± 0.004	0.15	0.5262	0.1660	0.0067	0.3012		77.275	29.687	29.495	0.65
NFS-12	1346	2.648 ± 0.015	0.57	0.4818	0.1674	0.0013	0.3495		77.436	29.243	29.139	0.36
NFS-12	1441	2.626 ± 0.013	0.50	0.4813	0.1665	0.0031	0.3491		77.367	29.462	29.364	0.33
NFS-12	1532	2.608 ± 0.012	0.46	0.4803	0.1647	0.0065	0.3484		77.220	29.609	29.540	0.23
NFS-12	1626	2.600 ± 0.007	0.27	0.4785	0.1616	0.0129	0.3471		76.996	29.614	29.675	–0.21
LC-25*	1639	2.592		0.6596	0.1526	0.0218	0.1660		75.855	29.265	29.049	0.74
LC-25*	1688	2.586		0.6574	0.1498	0.0274	0.1654		75.641	29.250	29.004	0.84
LC-25*	1734	2.581		0.6549	0.1467	0.0335	0.1648		75.397	29.212	28.945	0.91
KFS-2	1240	2.517		0.5016	0.1272	0.0006		0.3706	85.403	33.931	33.876	–0.16
KFS-2	1342	2.491		0.5013	0.1267	0.0015		0.3704	85.351	34.264	34.311	0.14
KFS-2	1440	2.469		0.5007	0.1258	0.0035		0.3700	85.277	34.539	34.708	0.49
KFS-2	1533	2.440		0.4998	0.1241	0.0068		0.3693	85.123	34.887	35.046	0.46
KFS-2	1625	2.416		0.4982	0.1214	0.0123		0.3681	84.878	35.132	35.327	0.56
KFS-3	1440	2.356		0.5577	0.0695	0.0018		0.3710	79.684	33.822	33.913	0.27
KFS-3	1533	2.323		0.5572	0.0686	0.0036		0.3706	79.602	34.267	34.289	0.06
KFS-4	1440	2.412		0.5821	0.0936	0.0022		0.3221	80.421	33.342	33.445	0.31
KFS-4	1533	2.386		0.5814	0.0925	0.0045		0.3217	80.331	33.668	33.759	0.27
KFS-4	1625	2.362		0.5802	0.0906	0.0081		0.3211	80.157	33.936	34.032	0.28
KFS-5	1440	2.308		0.6586	0.0451	0.0010		0.2954	74.671	32.353	32.298	–0.17
KFS-5	1533	2.275		0.6582	0.0446	0.0019		0.2952	74.613	32.797	32.604	–0.59
KFS-5	1625	2.258		0.6577	0.0438	0.0035		0.2950	74.551	33.016	32.901	–0.35
KFS-5	1716	2.243		0.6568	0.0426	0.0060		0.2946	74.447	33.191	33.171	–0.06
KFS-6	1440	2.403		0.6600	0.0854	0.0018		0.2529	77.245	32.145	32.172	0.08
KFS-6	1533	2.388		0.6393	0.0845	0.0035		0.2526	75.951	31.805	31.879	0.23
KFS-6	1625	2.368		0.6583	0.0831	0.0065		0.2522	77.047	32.537	32.634	0.30
KFS-6	1716	2.348		0.6566	0.0808	0.0110		0.2516	76.845	32.728	32.810	0.25

* The original density data are reported here because they were not reported in Lange and Carmichael (1987). The molar volumes for LC-25 at each temperature of measurement are slightly higher than those given in the Appendix of Lange and Carmichael (1987) because different ferric-ferrous ratios were calculated for each temperature of measurement.

average residual of ±0.36%. The largest residuals are within the range of the maximum estimated error in molar volume, and the average residual is of the same magnitude as the average experimental error in molar volume of ~0.4%. Therefore, within experimental resolution, $\overline{V}_{Fe_2O_3}$ appears to be independent of composition for the liquids examined in this study. A similar conclusion is drawn from the results from Dingwell et al. (1988). The residuals for 36 density measurements on 11 liquids at various temperatures range from +1.69 to –2.13%, with an average residual of 0.70%. The larger residuals (by a factor of ~2) can be attributed to the larger compositional errors for their experimental liquids (Table 1b), owing to the difference in the analytical method that was used (electron microprobe vs. wet chemistry). The totals for the analyses reported by Dingwell et al. (1988) indicate an average error of ~1.2% for their liquid gfw, which propagates to the derived molar volumes. Thus, there is no experimentally resolved compositional

TABLE 4. Comparison of four acmite liquids at 1673 K

Sample	NFS-10	DBD-2	LC-25	Mo-002
X_{SiO_2}	0.6446	0.6632	0.658	0.6561
$X_{Fe_2O_3}$	0.1532	0.1555	0.1508	0.1539
X_{FeO}	0.0249	0.0275	0.0255	0.0262
X_{Na_2O}	0.1773	0.1539	0.1656	0.1638
$X_{Na_2O}/X_{Fe_2O_3}$	1.16	0.99	1.10	1.06
gfw	75.973	76.194	75.713	76.032
Density (g/cm³)	2.610	2.614	2.588	2.574
Molar volume (cm³/mol)	29.108	29.149	29.255	29.539

TABLE 5. Model equation for iron-bearing alkali silicate liquids

Oxide component	$\overline{V}_i$ (1673 K) ±2σ cm³/mol	$\partial\overline{V}_i/\partial T$ ±2σ 10^{-3} cm³/mol-K
SiO_2	26.69 ± 0.14	–
Fe_2O_3	41.52 ± 0.34	–
FeO	13.92 ± 0.50	3.69 ± 4.18
Na_2O	29.23 ± 0.26	7.90 ± 0.46
K_2O	46.28 ± 0.36	12.16 ± 1.00

or temperature dependence to $\overline{V}_{Fe_2O_3}$ for the liquids used to calibrate Equation 2. Nonetheless, plots of the residuals as a function of alkali, silica, and total Fe concentration (Fig. 4) allow a closer evaluation of any possible compositional dependence.

Figures 4a and 4b show that there is no structure to the residuals as a function of either alkali or silica content. However, there does appear to be a slight systematic variation in the residuals for our NFS liquids (but not for those from Dingwell et al. 1988) as a function of total Fe concentration (Fig. 4c). This variation is of interest owing to the observation made by Lange and Carmichael (1989), for the sodic silicate liquids examined in their study, that values of Fe_2O_3/FeO increase with total Fe concentration, but are independent of Na_2O and SiO_2 concentration. If $\overline{V}_{Fe_2O_3}$ increases slightly with total Fe concentration, owing to an increase in the proportion of tetrahedral Fe^{3+}, then this may cause Fe_2O_3/FeO to increase as well (Nishida et al. 1981; Baiocchi et al. 1982; Mysen 1987; Hannoyer et al. 1992). However, this trend in the residuals (Fig. 4c) is not outside experimental error, and is only observed for the data from the present study.

To test the compositional dependence to $\overline{V}_{Fe_2O_3}$ more directly, the four liquids from this study (NFS-9, -10, -11, -12) as well as the two liquids from Dingwell et al. (1988) (DBD-2, -5) with the same total Fe concentration (~16.8 ± 0.2 mol%), but different Na:Si ratios, were added independently to the Fe_2O_3-free data set in a series of regressions of Equation 2 to derive $\overline{V}_{Fe_2O_3}$ for each liquid. For these liquids, the fitted values for $\partial\overline{V}_{Fe_2O_3}/\partial T$ were indistinguishable from zero. The results are presented in Figure 5a as a function of Na_2O concentration, and the data show that $\overline{V}_{Fe_2O_3}$ does not vary systematically with variations in the Na:Si ratio. The most robust conclusion, therefore, is that $\overline{V}_{Fe_2O_3}$ is independent of composition and temperature in peralkaline silicate liquids. The best estimate for the value of $\overline{V}_{Fe_2O_3}$ is that obtained from the linear fit, namely 41.52 ± 0.34 cm³/mol.

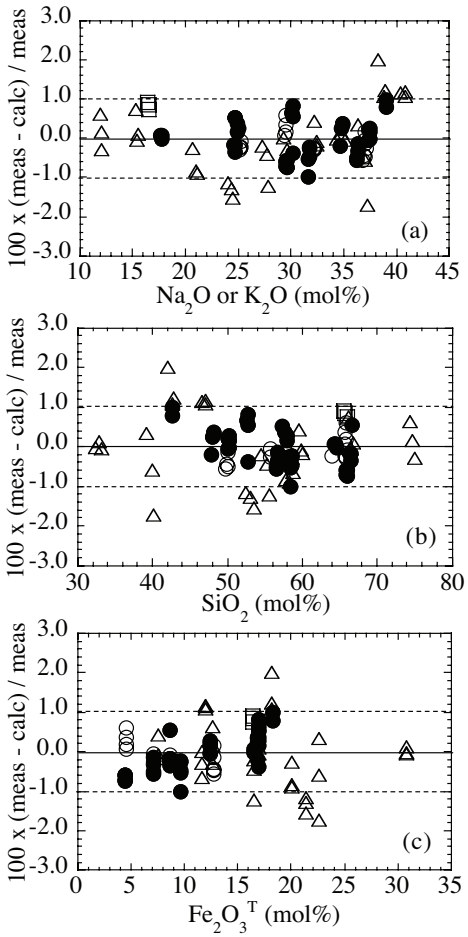

FIGURE 4. The residuals plotted as a function of composition (in mol%): (**a**) Na_2O, (**b**) SiO_2, (**c**) Fe_2O_3 (total). The values of NFS samples from this study are shown as solid circles, the KFS samples from this study are shown as open circles, NFS samples from Dingwell et al. (1988) are shown as open triangles, and LC-25 from Lange and Carmichael (1987) are shown as open squares.

DISCUSSION

Topological mechanisms vs. Fe^{3+} coordination change to explain the value for $\overline{V}_{Fe_2O_3}$

There are two mechanisms by which the oxide partial molar volumes of network formers (e.g., Si^{4+}, Al^{3+}, Ti^{4+}, Fe^{3+}) in multicomponent silicate liquids may change as a function of temperature, pressure, and composition. One involves coordination change of the network-forming cation (4 vs. 5 vs. 6), whereas the other is topological and may involve changes in Q^n speciation, T-O-T bond angles, and network connectivity, such as the occurrence of clusters and/or changes in the size distribution of rings of tetrahedra. For example, Stixrude and Bukowinski (1990a) demonstrated that topological variations in network connectivity can exert a strong influence on melt density. Using Monte-Carlo simulations of tetrahedrally bonded SiO_2 liquid at various pressures, they showed that SiO_2 melt compresses by reducing the abundance of three-membered rings in favor of larger-sized rings and a broader distribution of the size of rings. These conclusions are consistent with the strong variations in density (factor of 2) observed in crystalline frameworks as a systematic function of ring statistics (Stixrude and Bukowinski 1990b), where decreasing ring size leads to lower density. The gradual increase in ring size seen in the simulated liquids with pressure is achieved only because Si-O bonds are constantly broken and reformed;

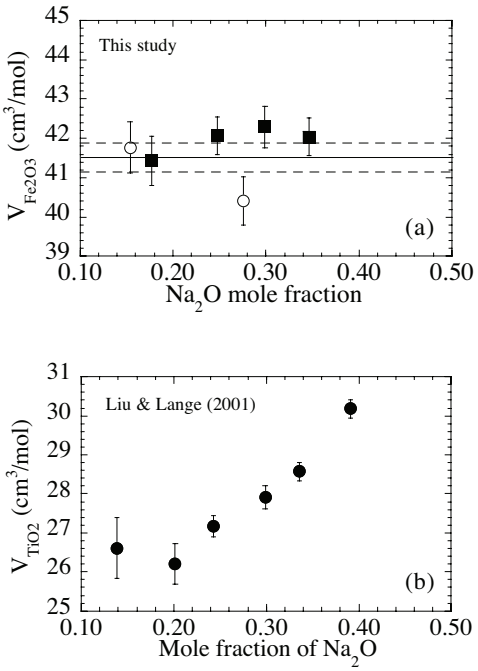

FIGURE 5. A comparison plot of (**a**) $\overline{V}_{Fe_2O_3}$ ($\pm 2\sigma$) vs. Na_2O concentration for NFS liquids with similar total Fe concentration (~16.8 ± 0.2 mol%), and varied Na:Si ratio (NFS-9, -10, -11, –12 from this study, solid squares; DBD-2, -5 from Dingwell et al. 1988, open circles). The solid line and dashed lines show the compositionally independent $\overline{V}_{Fe_2O_3}$ (41.52 ± 0.34), and (**b**) $\overline{V}_{TiO_2}$ ($\pm 2\sigma$) at 1573 K vs. Na_2O mole fraction for the six NTS liquids from Liu and Lange (2001) with similar TiO_2 concentration (~25 mol%), but different Na:Si ratio.

therefore, it is a compression mechanism uniquely available to liquids and not crystals. This may be an important topological mechanism for the compression of silicate liquids at moderate pressures (e.g., rhyolite liquid to 3 GPa, Gaetani et al. 1998; $NaAlSi_3O_8$ liquid to ~8 GPa, Lee et al. 2004), where neither Si^{4+} nor Al^{3+} undergoes a coordination change.

In the case of $\overline{V}_{Fe_2O_3}$ in alkaline silicate melts at one bar, there does not appear to be any resolvable shift in its value as a function of either temperature or composition. This suggests that there are neither topological nor coordination-change mechanisms causing a change in $\overline{V}_{Fe_2O_3}$ on these liquids. Despite the lack of evidence for any resolvable variation in $\overline{V}_{Fe_2O_3}$ induced by either increasing temperature or changing composition (e.g., a variable Na:Si ratio at constant total Fe concentration), the question still arises as to what is the average coordination number for Fe^{3+} in these alkaline silicate liquids when the derived value for $\overline{V}_{Fe_2O_3}$ is ~41.5 cm^3/mol. To evaluate this question, it is necessary to first review what is known about the coordination of Fe^{3+} in silicate liquids.

Fe^{3+} coordination in silicate melts

Fe^{3+} is known to be four-, five-, and sixfold coordinated in various minerals, although the relative abundance of these three coordination states for Fe^{3+} in silicate melts, and how they vary with composition, is not well known. Hannoyer et al. (1992) provided a summary of published estimates of Fe^{3+} coordination numbers in different alkali silicate and soda-lime silicate glasses, obtained by a variety of methods including optical, electron paramagnetic resonance, and Mössbauer spectroscopic methods, as well as XANES and extended XAFS spectroscopy. Most of these studies conclude that Fe^{3+} is predominantly in tetrahedral coordination in alkali and soda-lime silicate glasses (e.g., Steele and Douglas 1965; Kurkjian and Sigety 1968; Hirao et al. 1979; Fox et al. 1982; Greaves et al. 1984; Brown et al. 1986; Wang et al. 1993, 1995). However, other studies have concluded that both tetrahedral and octahedral Fe^{3+} are present in alkali silicate and soda-lime silicate glasses (e.g., Levy et al. 1976; de Grae 1980; Fenstermacher 1980; Calas and Petiau 1983; Wang and Chen 1987; Hannoyer et al. 1992). There is also Mössbauer evidence that Fe^{3+} may be present in pentacoordinated sites in some silicate glasses and melts, including those of acmite ($NaFeSi_2O_6$) composition (Bychkov et al. 1993). Although it is difficult to distinguish between a single population of $^{V}Fe^{3+}$ and a combined population of $^{IV}Fe^{3+}$ and $^{VI}Fe^{3+}$ from Mössbauer spectra, $^{V}Fe^{3+}$ is known to occur in a few silicate minerals, including vesuvianite (Olesch 1979), andalusite (Abswurmbach et al. 1981), yoderite (Higgins et al. 1982), and orthoericssonite (Halenius 1995).

Recently, the first unequivocal report of $^{V}Fe^{3+}$ in silicate glasses was made by Farges et al. (2004) on the basis of a combined study of XAFS spectroscopy and MD simulations. Their estimated average coordination number for Fe^{3+} in their sample glasses (27 within the SiO_2-Al_2O_3-Fe_2O_3-FeO-MgO-CaO-Na_2O-K_2O system) ranges from 4.4 to 4.8, and their MD simulations found no evidence for significant concentrations of $^{VI}Fe^{3+}$. The latter observation strongly supports the presence of five-coordinated Fe^{3+} sites (and not just a combination of $^{IV}Fe^{3+}$ and $^{VI}Fe^{3+}$) in these silicate glasses.

$\overline{V}_{Fe_2O_3}$ and Fe^{3+} coordination

It is of interest to estimate the value of $\overline{V}_{Fe_2O_3}$ in silicate melts under the end-member conditions of Fe^{3+} in fourfold vs. sixfold coordination, and from this to derive the average Fe^{3+} coordination number for the fitted value for $\overline{V}_{Fe_2O_3}$ of 41.5 cm^3/mol. Here, we elaborate on the method outlined in Lange and Carmichael (1990) to estimate the value of $\overline{V}_{Fe_2O_3}$ when Fe^{3+} is entirely in tetrahedral coordination. We begin by taking the 298 K crystalline volumes of $KAlSi_3O_8$ (108.84 cm^3/mol; Ferguson et al. 1991) and $KFeSi_3O_8$ (112.40 cm^3/mol; Bychkov et al. 1998), where both Al^{3+} and Fe^{3+} are in tetrahedral coordination, and obtain their ratio of 0.968. Next, we calculate what value for $\overline{V}_{Fe_2O_3}$ maintains this ratio of 0.968 for the liquid components: $KAlSi_3O_8$ /$KFeSi_3O_8$ at 1673 K. From the partial molar volume data provided by Lange (1997), the calculated value is ~45.5 ± 1 cm^3/mol, which is our best estimate for $\overline{V}_{Fe_2O_3}$ when Fe^{3+} is entirely in tetrahedral coordination. For Fe^{3+} entirely in octahedral coordination, we begin with the volume of crystalline hematite at 1673 K (31.98 cm^3/mol; Robie and Hemingway 1995; Taylor 1984). If the volume of fusion for hematite is assumed to be ~5–10% (to a hypothetical pure Fe_2O_3 liquid in which all the Fe^{3+} is sixfold coordinated), then $\overline{V}_{Fe_2O_3}$ takes a value of ~34 ± 1 cm^3/mol in this end-member case.

If we further assume that $\overline{V}_{Fe_2O_3}$ varies linearly with Fe^{3+} coordination, then the average Fe^{3+} coordination number can

be calculated for the fitted value of $\overline{V}_{Fe_2O_3}$ from the regression of Equation 1. Within the error for the estimated end-members, the average Fe^{3+} coordination number is calculated to be between 4.5 and 5.0 for $\overline{V}_{Fe_2O_3}$ = 41.5 cm^3/mol. Although there is some error built into this calculation, the broad conclusion that the average coordination of Fe^{3+} is intermediate between 4 and 5 in these alkaline silicate liquids is robust. Moreover, it can be tested by XAFS spectroscopy and MD simulations, as performed by Farges et al. (2004).

Comparison with Ti-bearing alkali silicate liquids

Compositional dependence to $\overline{V}_{Fe_2O_3}$ and $\overline{V}_{TiO_2}$. Despite the capacity for both Ti^{4+} and Fe^{3+} to occur in four-, five-, and sixfold coordination sites, the pattern of compositional dependence of $\overline{V}_{Fe_2O_3}$ and $\overline{V}_{TiO_2}$ in alkali silicate liquids is strikingly different. Liu and Lange (2001) showed that $\overline{V}_{TiO_2}$ varies strongly and linearly as a function of alkali concentration, which is in marked contrast to the pattern observed for $\overline{V}_{Fe_2O_3}$ in this study (Fig. 5a). In Figure 5b, fitted values of $\overline{V}_{TiO_2}$ are shown for six liquids from Liu and Lange (2001), which have the same TiO_2 concentration (~25 mol%), but different Na:Si ratios. For these six liquids, $\overline{V}_{TiO_2}$ increases strongly and linearly with Na_2O concentration.

Another difference between what is observed for $\overline{V}_{Fe_2O_3}$ vs. $\overline{V}_{TiO_2}$ in alkaline silicate liquids is the lack of any difference in the value for $\overline{V}_{Fe_2O_3}$ between Na- and K-bearing liquids. In contrast, the value for $\overline{V}_{TiO_2}$ is ~3 cm^3/mol smaller in sodic vs. potassic liquids at equivalent bulk composition (Liu and Lange 2001), which reflects an increase in the average Ti^{4+} coordination of ~0.6 in sodic vs. potassic liquids. This is exactly what is expected on the basis of bond-valence models, as discussed by Liu and Lange (2001) and Farges et al. (1996b). For example, when K is replaced by Na, the contribution of the alkalis to the bond-valence sum increases, owing to the longer K-O distance (2.9 Å) vs. Na-O distance (2.6 Å) and the lower average coordination of Na vs. that for K. This increase in the bond-valence sum is compensated if the Ti-O bond length sum lengthens, which is achieved if the Ti coordination increases.

Temperature dependence to $\overline{V}_{Fe_2O_3}$ and $\overline{V}_{TiO_2}$ and topological mechanisms of expansion. Perhaps the most striking difference between the behavior of $\overline{V}_{Fe_2O_3}$ and $\overline{V}_{TiO_2}$ resides with their respective temperature dependence in the stable liquid region. Within 2σ error, $\partial\overline{V}_{Fe_2O_3}/\partial T$ is indistinguishable from zero for all the liquids examined in this study. In contrast, Figure 6 shows $\partial\overline{V}_{TiO_2}/\partial T$ plotted as a function of $\overline{V}_{TiO_2}$. As pointed out by Liu and Lange (2001), $\partial\overline{V}_{TiO_2}/\partial T$ is near zero when $\overline{V}_{TiO_2}$ is ~32.5 cm^3/mol (when Ti^{4+} is predominantly in tetrahedral coordination) and reaches a maximum of ~8×10^{-3} cm^3/mol-K when $\overline{V}_{TiO_2}$ is ~26 cm^3/mol (when the average Ti^{4+} coordination is near 5).

A negligible thermal expansivity for $\partial\overline{V}_{Fe_2O_3}/\partial T$ is similar to what is found for the liquid SiO_2 and Al_2O_3 components (Lange 1997), where Si^{4+} and Al^{3+} are network-forming cations in tetrahedral coordination, and it is consistent with the zero value for $\partial\overline{V}_{TiO_2}/\partial T$ when Ti^{4+} is in tetrahedral coordination. Liu and Lange (2001) showed that the increase in $\partial\overline{V}_{TiO_2}/\partial T$ may be related to an increase in the abundance of ^{V}Ti. The large value of $\partial\overline{V}_{TiO_2}/\partial T$ is unlikely to be caused by a shift in Ti^{4+} coordination (toward lower values) with increasing temperature, because this hypothesis was specifically tested and rejected in a variety of high-temperature spectroscopic studies (e.g., Mysen and Neuville 1995; Farges et al. 1996c; Reynard and Webb 1998). Instead, the increase in liquid thermal expansion is more likely the result of topological changes that appear to be enhanced when the average Ti^{4+} coordination number is near five. The results of this study show that this does not appear to be the case when the average Fe^{3+} coordination is near five.

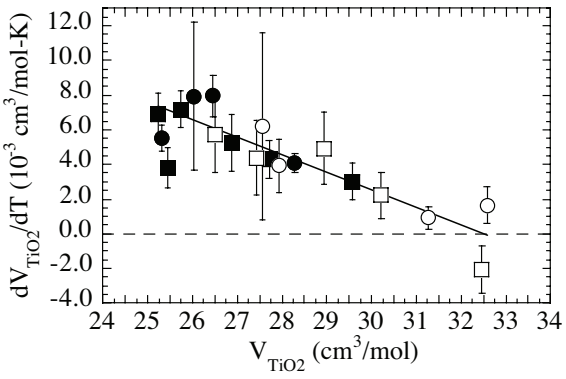

FIGURE 6. $\partial\overline{V}_{TiO_2}/\partial T$ (±1σ) plotted as a function of $\overline{V}_{TiO_2}$ at 1373 K. Solid symbols represent NTS liquids, open symbols refer to KTS liquids. Six NTS and five KTS liquids with similar TiO_2 concentration (~25 mol%) are shown as squares. The other liquids are shown as circles. Data are taken from Liu and Lange (2001).

Different coordination geometries for five-coordinated Ti^{4+} and Fe^{3+}. The cause of the strikingly different behavior in the thermal expansion and compositional dependence for $\overline{V}_{Fe_2O_3}$ vs. $\overline{V}_{TiO_2}$ may relate to the different coordination geometries for $^{V}Fe^{3+}$ vs. $^{V}Ti^{4+}$ in alkali silicate liquids. Through a series of Ti *K*-edge XAFS spectroscopic studies, Farges et al. (1996b, 1996c) found that $^{V}Ti^{4+}$ is present in alkali silicate glasses as titanyl square pyramids with one non-bridging O atom doubly bonded to Ti (and four alkali cations) and four bridging O atoms bonded to Si or Ti (and two other alkali cations). As a consequence of this geometry, ^{V}Ti occurs at the interface of two domains, one that is relatively rich in alkalis (percolation domains) and the other that is rich in silica (network formers). This geometry for ^{V}Ti may explain why its relative abundance is so sensitive to the ratio of Na:Si in the melt. Moreover, the occurrence of percolation domains may lead to novel topological mechanisms of expansion that are otherwise unavailable in alkali silicate liquids.

In contrast, on the basis of EXAFS spectra and MD simulations, Farges et al. (2004) show that $^{V}Fe^{3+}$ occurs in trigonal bipyramidal sites. This is also the most common site for $^{V}Al^{3+}$ in various minerals (e.g., andalusite; Burnham and Buerger 1961). It is unlikely that a symmetric, undistorted trigonal bipyramidal site for a five-coordinated cation would produce percolation domains in alkali silicate liquids as has been documented for the square pyramidal site for $^{V}Ti^{4+}$ (Farges et al. 1996b, 1996c). If this best describes the geometry for $^{V}Fe^{3+}$, then $^{V}Fe^{3+}$-bearing alkali silicate liquids may not have the same topological mechanisms of expansion as $^{V}Ti^{4+}$-bearing liquids, and the relative abundance of $^{V}Fe^{3+}$ may not be as sensitive to the Na:Si ratio in the melt. At the present time, this hypothesis is purely speculative and requires further research to verify. But the role of a different geometry for $^{V}Fe^{3+}$ vs. $^{V}Ti^{4+}$ in controlling the compositional

and temperature dependence to $\overline{V}_{Fe_2O_3}$ vs. $\overline{V}_{TiO_2}$ in alkali silicate liquids is a testable hypothesis that future spectroscopic studies and molecular dynamic simulations can address.

ACKNOWLEDGMENTS

This research was supported by the National Science Foundation (EAR-0440097). Discussions with Lars Stixrude and thoughtful reviews by Sung Keun Lee and Victor Kress considerably improved the manuscript.

REFERENCES CITED

Abswurmbach, I., Langer, K., Seifert, F., and Tillmanns, E. (1981) The crystal-chemistry of (Mn^{3+},Fe^{3+})-substituted andalusites (viridines and kanonaite), ($Al_{1-x-y}Mn_x^{3+}Fe_y^{x+}$)$_2$-(O-$SiO_4$): Crystal-structure refinements, Mössbauer, and polarized optical-absorption spectra. Zeitschrift für Kristallographie, 155, 81–113.

Baiocchi, E., Bettinelli, M., Montenero, A., and Disipio, L. (1982) Spectroscopic behavior of iron(Iii) in silicate glass. Journal of the American Ceramic Society, 65, C39–C40.

Bockris, J.O., Tomlinson, J.W., and White, J.L. (1956) The structure of the liquid silicates - partial molar volumes and expansivities. Transactions of the Faraday Society, 52, 299–310.

Bouhifd, M.A., Sipp, A., and Richet, P. (1999) Heat capacity, viscosity, and configurational entropy of alkali titanosilicate melts. Geochimica et Cosmochimica Acta, 63, 2429–2437.

Brown, G.E., Jr., Waychunas, G.A., Ponader, C.W., Jackson, W.E., and McKeown, D.A. (1986) EXAFS and NEXAFS studies of cation environments in oxide glasses. Journal de Physique. Colloque (Paris), 47, 661–668.

Burnham, C.W. and Buerger, M.J. (1961) Refinement of the crystal structure of andalusite. Zeitschrift fuer Kristallographie, 115, 269–290.

Bychkov, A.M., Borisov, A.A., Khramov, D.A., and Urusov, V.S. (1993) Change in the immediate environment of Fe atoms during the melting of minerals. Geochemistry International, 30, 1–25.

Bychkov, A.M., Rusakov, V.S., Chistyakova, N.I., Kuz'mina, N.A., and Urusov, V.S. (1998) Ordering kinetics in ferric feldspars exposed to low-temperature hydrothermal conditions: An x-ray and Mössbauer study. Geochemistry International, 36, 517–522.

Calas, G. and Petiau, J. (1983) Coordination of iron in oxide glasses through high-resolution K-edge spectra—information from the pre-edge. Solid State Communications, 48, 625–629.

Carmichael, I.S.E. (1991) The redox states of basic and silicic magmas: A reflection of their source regions. Contributions to Mineralogy and Petrology, 106, 129–141.

de Grave, E., Chambaere, D., van Iseghem, P., and de Batist, R. (1980) Mössbauer spectroscopic study of some complex M_2O-MO-M_2O_3-SiO_2 glasses. Journal de Physique. Colloque (Paris), 41, 269–270.

Dingwell, D.B., Brearley, M., and Dickinson, J.E. (1988) Melt densities in the Na_2O-FeO-Fe_2O_3-SiO_2 system and the partial molar volume of tetrahedrally-coordinated ferric iron in silicate melts. Geochimica et Cosmochimica Acta, 52, 2467–2475.

Farges, F. (1997) Coordination of Ti^{4+} in silicate glasses: A high resolution XANES spectroscopic study at the Ti K edge. American Mineralogist, 82, 36–43.

Farges, F., Brown, G.E., Jr., and Rehr, J.J. (1996a) Coordination chemistry of Ti(IV) in silicate glasses and melts: 1. XAFS study of titanium coordination in oxide model compounds. Geochimica et Cosmochimica Acta, 60, 3023–3038.

Farges, F., Brown, G.E., Jr., Navrotsky, A., Gan, H., and Rehr, J.J. (1996b) Coordination chemistry of Ti(IV) in silicate glasses and melts: II. Glasses at ambient temperature and pressure. Geochimica et Cosmochimica Acta, 60, 3039–3053.

——— (1996c) Coordination chemistry of Ti(IV) in silicate glasses and melts: III. Glasses and melts from ambient to high temperatures. Geochimica et Cosmochimica Acta, 60, 3055–3065.

Farges, F., Lefrere, Y., Rossano, S., Berthereau, A., Calas, G., and Brown, G.E., Jr. (2004) The effect of redox state on the local structural environment of iron in silicate glasses: A molecular dynamics, combined XAFS spectroscopy, and bond valence study. Journal of Non-Crystalline Solids, 344, 176–188.

Fenstermacher, J.E. (1980) Optical-absorption due to tetrahedral and octahedral ferric iron in silicate-glasses. Journal of Non-Crystalline Solids, 38–9, 239–244.

Ferguson, R.B., Ball, N.A., and Cerny, P. (1991) Structure refinement of an adularian end-member high sanidine from the buck claim pegmatite, Bernic Lake, Manitoba. Canadian Mineralogist, 29, 543–552.

Fox, K.E., Furukawa, T., and White, W.B. (1982) Transition-metal ions in silicate melts. 2. Iron in sodium-silicate glasses. Physics and Chemistry of Glasses, 23, 169–178.

Gaetani, G.A., Asimow, P.D., and Stolper, E.M. (1998) Determination of the partial molar volume of SiO_2 in silicate liquids at elevated pressures and temperatures: A new experimental approach. Geochimica et Cosmochimica Acta, 62, 2499–2508.

Greaves, G.N., Binsted, N., and Henderson, C.M.B. (1984) The environment of modifiers in oxide glasses. In K.O. Hodgson, B. Hedman, and J.E. Penner-Haln, Eds., EXAFS and Near Edge Structure III: Proceedings of an international conference, p. 297–301. Springer-Verlag, New York.

Halenius, U. (1995) A Mössbauer study of pentacoordinated ferric iron in orthoericssonite. Mineralogical Journal, 17, 363–371.

Hannoyer, B., Lenglet, M., Durr, J., and Cortes, R. (1992) Spectroscopic evidence of octahedral iron(III) in soda-lime silicate-glasses. Journal of Non-Crystalline Solids, 151, 209–216.

Higgins, J.B., Ribbe, P.H., and Nakajima, Y. (1982) An ordering model for the commensurate antiphase structure of yoderite. American Mineralogist, 67, 76–84.

Hirao, K., Soga, N., and Kunugi, M. (1979) Mössbauer and ESR analyses of the distribution of Fe^{3+} in leucite-type iron silicate-glasses and crystals. Journal of the American Ceramic Society, 62, 109–110.

Janz, G.J. (1980) Molten-salts data as reference-standards for density, surface-tension viscosity and electrical conductance—KNO_3 and NaCl. Journal of physical and chemical reference data, 9, 791–829.

Kress, V.C. and Carmichael, I.S.E. (1988) Stoichiometry of the iron oxidation reaction in silicate melts. American Mineralogist, 73, 1267–1274.

——— (1989) The lime-iron-silicate melt system — Redox and volume systematics. Geochimica et Cosmochimica Acta, 53, 2883–2892.

——— (1991) The compressibility of silicate liquids containing Fe_2O_3 and the effect of composition, temperature, oxygen fugacity and pressure on their redox states. Contributions to Mineralogy and Petrology, 108, 82–92.

Kurkjian, C.R. and Sigety, E.A. (1968) Co-ordination of Fe^{3+} in glass. Physics and Chemistry of Glasses, 9, 73–83.

Lange, R.A. (1996) Temperature independent thermal expansivities of sodium aluminosilicate melts between 713 and 1835 K. Geochimica et Cosmochimica Acta, 60, 4989–4996.

——— (1997) A revised model for the density and thermal expansivity of K_2O-Na_2O-CaO-MgO-Al_2O_3-SiO_2 liquids from 700 to 1900 K: Extension to crustal magmatic temperatures. Contributions to Mineralogy and Petrology, 130, 1–11.

Lange, R.A. and Carmichael, I.S.E. (1987) Densities of Na_2O-K_2O-CaO-MgO-FeO-Fe_2O_3-Al_2O_3-TiO_2-SiO_2 liquids: New measurements and derived partial molar properties. Geochimica et Cosmochimica Acta, 51, 2931–2946.

——— (1989) Ferric-ferrous equilibria in Na_2O-FeO-Fe_2O_3-SiO_2 melts: Effects of analytical techniques on derived partial molar volumes. Geochimica et Cosmochimica Acta, 53, 2195–2204.

——— (1990) Thermodynamic properties of silicate liquids with emphasis on density, thermal-expansion and compressibility. In J. Nicholls and J.K. Russell, Eds., Modern Methods of Igneous Petrology: Understanding Magmatic Processes, 24, 25–64. Reviews in Mineralogy, Mineralogical Society of America, Chantilly, Virginia.

Lange, R.A. and Navrotsky, A. (1993) Heat-Capacities of TiO_2-bearing silicate liquids—Evidence for anomalous changes in configurational entropy with temperature. Geochimica et Cosmochimica Acta, 57, 3001–3011.

Lee, S.K., Cody, G.D., Fei, Y.W., and Mysen, B.O. (2004) Nature of polymerization and properties of silicate melts and glasses at high pressure. Geochimica et Cosmochimica Acta, 68, 4189–4200.

Levy, R.A., Lupis, C.H.P., and Flinn, P.A. (1976) Mössbauer analysis of valence and coordination of iron cations in SiO_2-Na_2O-CaO glasses. Physics and Chemistry of Glasses, 17, 94–103.

Liu, Q. and Lange, R.A. (2001) The partial molar volume and thermal expansivity of TiO_2 in alkali silicate melts: Systematic variation with Ti coordination. Geochimica et Cosmochimica Acta, 65, 2379–2393.

Mo, X., Carmichael, I.S.E., Rivers, M., and Stebbins, J.F. (1982) The partial molar volume of Fe_2O_3 in multicomponent silicate liquids and the pressure-dependence of oxygen fugacity in magmas. Mineralogical Magazine, 45, 237–245.

Mysen, B.O. (1987) Redox Equilibria and Coordination of Fe^{2+} and Fe^{3+} in Silicate-Glasses from Fe-57 Mössbauer-Spectroscopy. Journal of Non-Crystalline Solids, 95–6, 247–254.

Mysen, B. and Neuville, D. (1995) Effect of temperature and TiO_2 content on the structure of $Na_2Si_2O_5$-$Na_2Ti_2O_5$ melts and glasses. Geochimica et Cosmochimica Acta, 59, 325–342.

Nishida, K., Tani, T., Narita, T., and Ohashi, H. (1981) A Mössbauer spectroscopic study of sulfidation of iron-manganese alloys. Corrosion Science, 21, 627–637.

Olesch, M. (1979) Naturliche und synthetische Fe-haltige Vesuviane. Fortschritte der Mineralogie, 57, 114–115.

Reynard, B. and Webb, S.L. (1998) High-temperature Raman spectroscopy of $Na_2TiSi_2O_7$ glass and melt: Coordination of Ti^{4+} and nature of the configurational changes in the liquid. European Journal of Mineralogy, 10, 49–58.

Richet, P. and Bottinga, Y. (1985) Heat-capacity of aluminum-free liquid silicates. Geochimica et Cosmochimica Acta, 49, 471–486.

Robie, R.A. and Hemingway, B.S. (1995) Thermodynamic properties of minerals and related substances at 298.15 K and 1 bar (10^5 pascals) pressure and at

higher temperatures. U.S. Geological Survey Bulletin, 2131.
Sack, R.O., Carmichael, I.S.E., Rivers, M., and Ghiorso, M.S. (1980) Ferric-ferrous equilibria in natural silicate liquids at 1 bar. Contributions to Mineralogy and Petrology, 75, 369–376.
Steele, F.N. and Douglas, R.W. (1965) Some observations on absorption of iron in silicate and borate glasses. Physics and Chemistry of Glasses, 6, 246–252.
Stein, D.J., Stebbins, J.F., and Carmichael, I.S.E. (1986) Density of molten sodium aluminosilicates. Journal of the American Ceramic Society, 69, 396–399.
Stixrude, L. and Bukowinski, M.S.T. (1990a) A Novel topological compression mechanism in a covalent liquid. Science, 250, 541–543.
——— (1990b) Rings, topology, and the density of tectosilicates. American Mineralogist, 75, 1159–1169.
Tangeman, J.A. and Lange, R.A. (1998) The effect of Al^{3+}, Fe^{3+} and Ti^{4+} on the configurational heat capacities of sodium silicate liquids. Physics and Chemistry of Minerals, 26, 83–99.
Tangeman, J.A., Lange, R., and Forman, L. (2001) Ferric-ferrous equilibria in K_2O-FeO-Fe_2O_3-SiO_2 melts. Geochimica et Cosmochimica Acta, 65, 1809–1819.
Taylor, D. (1984) Thermal expansion data: IV. Binary oxides with the silica structures. British Ceramic, Transactions and Journal, 83, 129–134.
Thornber, C.R., Roeder, P.L., and Foster, J.R. (1980) The effect of composition on the ferric-ferrous ratio in basaltic liquids at atmospheric pressure. Geochimica et Cosmochimica Acta, 44, 525–532.
Wang, C.M. and Chen, H. (1987) Mixed coordination of Fe^{3+} and its dependence on the iron content in sodium disilicate glasses. Physics and Chemistry of Glasses, 28, 39–47.
Wang, Z.F., Cooney, T.F., and Sharma, S.K. (1993) High-temperature structural investigation of $Na_2O{\cdot}0.5Fe_2O_3{\cdot}3SiO_2$ and $Na_2O{\cdot}FeO{\cdot}3SiO_2$ melts and glasses. Contributions to Mineralogy and Petrology, 115, 112–122.
——— (1995) In-situ structural investigation of iron-containing silicate liquids and glasses. Geochimica et Cosmochimica Acta, 59, 1571–1577.

MANUSCRIPT RECEIVED JANUARY 27, 2005
MANUSCRIPT ACCEPTED AUGUST 1, 2005
MANUSCRIPT HANDLED BY PAUL ASIMOW